Etching, Insertion, and Abstraction Reactions of Atomic Deuterium with Amorphous Silicon Hydride Films

C.-M. Chiang and S. M. Gates*

IBM T. J. Watson Research Center, Yorktown Hts., New York 10598

Szetsen S. Lee, M. Kong, and Stacey F. Bent

Department of Chemistry, New York University, New York, New York, 10003

Received: November 6, 1996; In Final Form: September 11, 1997[⊗]

We report structural and kinetic studies of the reactions of hydride species in Si thin films with atomic deuterium (D_{at}). Infrared (IR) spectroscopy is used to obtain Si−H bonding information, and direct recoiling methods are used to measure reaction rates. Two kinds of films are prepared by filament-assisted growth from Si_2H_6 and are characterized by IR spectroscopy. A film containing only monohydride hydrogen is grown at 200 °C, and a polymer containing tri-, di-, and monohydride is grown at −110 °C. Rates of H abstraction by D_{at}, and of D_{at} insertion into Si−Si bonds, are reported. The abstraction rate of H by D_{at} in both films is similar to the abstraction rate on H-terminated crystal Si surfaces. The insertion rate into Si−Si bonds in both films is about one-tenth the rate of abstraction. A qualitative study of the etching reaction of D_{at} with the polymeric film is reported, and a strong temperature dependence is observed.

I. Introduction

Chemistry of atoms on semiconductor surfaces is an area where plasma processing and fundamental studies of surface reactions converge. The silicon + atomic hydrogen system is a well-studied example of this convergence. Thin films of amorphous hydrogenated Si (a-Si:H) are deposited by plasma-enhanced (PE) chemical vapor deposition (CVD) for several applications, and many properties of this useful material depend on the amount of hydrogen bonded in the bulk of the film.[1,2] The surface reactions of atomic H (H_{at}) during PE CVD film growth influence the concentration and bonding of H in the a-Si:H film.[1] Cleaning of Si surfaces using H_2 plasmas has also been investigated.[3−5] The mechanisms and dynamics involved in the reactions of H_{at} on metal[6−8] and Si[9−14] surfaces are fundamentally intriguing. Mounting evidence for direct, Eley−Rideal (ER), abstraction reactions of H_{at} is of interest.[9−14] Here, we further define the kinetics of different reaction pathways for H_{at} reactions with Si films. We study the monohydride on the surface of a polycrystalline thin film and a mixture of the higher hydrides SiH_2 and SiH_3 in a heavily hydrogenated film, which we call "polysilane". Use of these two films prepared in situ allows the reactivity of the three hydrides to be studied under identical conditions. This comparison is not possible using single-crystal Si surfaces or a-Si:H films. We address the question, What are the mechanisms by which H_{at} improves the film quality in low-temperature PE CVD of a-Si:H?

Electronic quality a-Si:H is typically deposited using a pure SiH_4 plasma, on an amorphous substrate (glass) held at 270−420 °C. The bandgap, photoconductivity, dark conductivity, and stability of a-Si:H depend on the bulk H content, with optimum properties found at 15−25 atomic % H.[1,2,15] However, a pure SiH_4 plasma and 100 °C growth yields highly defective material.[15] Low growth temperatures (≈100 °C) require the addition of H_2 for high-quality material.[16,17] Near 100 °C, the dangling bond density (measured by electron spin resonance) is decreased with an H_2/SiH_4 ratio of 1−10.[17] We want to understand these effects. At the conventional T (300 ± 50 °C), if the H_2/SiH_4 ratio is increased to the range of 30−100, crystalline films are deposited, rather than a-Si:H,[1,16,18] another intriguing effect of hydrogen addition. The films consist of small crystallites, 30−500 Å in diameter. A few atomic % of hydrogen is bonded at the crystallite surfaces, and the material is known as "microcrystalline Si" (μc-Si),[1] simply a polycrystalline film with very small grain size, and with H termination of these grains.

Alternatively, exposure of an a-Si:H film to H_{at} *after film growth* causes related changes. Smaller H_{at} exposures *decrease* the bulk H content.[19] Larger H_{at} exposures convert the amorphous film to μc-Si.[20,21] Wronski, Collins, and co-workers demonstrated that etching and crystallization both occur, with the film thickness reduced by about 10 times in the μc-Si product film compared to the initial a-Si:H film.[20,21] The term "chemical annealing" has been used to describe these H_{at}-induced effects on a-Si:H.[19,22] Thicker films of μc-Si are made by alternating a-Si:H growth with H_{at} exposure using pulsed values.[18]

The fundamental reactions of H_{at} on crystal Si surfaces have been investigated by many groups and reviewed by Boland.[12] Chabal pioneered the use of multiple internal reflection Fourier transform infrared absorption spectroscopy (hereafter called "MIR-FTIR") and has studied the H + Si system extensively.[23−25] Much of our knowledge of the details of the mono-, di-, and trihydride species comes from MIR-FTIR.[23−29] Scanning tunneling microscopy (STM)[12] and mass spectrometry[30] have revealed other details. Figure 1 shows four classes of reaction that are known for atomic hydrogen or deuterium (D_{at}) interacting with a Si surface or film. Using the symbol _−Si for a dangling bond, we write reactions 1−3 for addition, abstraction, and insertion (see Figure 1).

$$D_{at} + \_-Si \rightarrow D-Si \quad (1)$$

$$D_{at} + H-Si \rightarrow H-D(g) + \_-Si \quad (2)$$

$$D_{at} + Si-Si \rightarrow D-Si + \_-Si \quad (3)$$

In Figure 1, we show only one example of an etching reaction

* Corresponding author.

[⊗] Abstract published in *Advance ACS Abstracts,* November 1, 1997.

S1089-5647(96)03717-0 CCC: $14.00

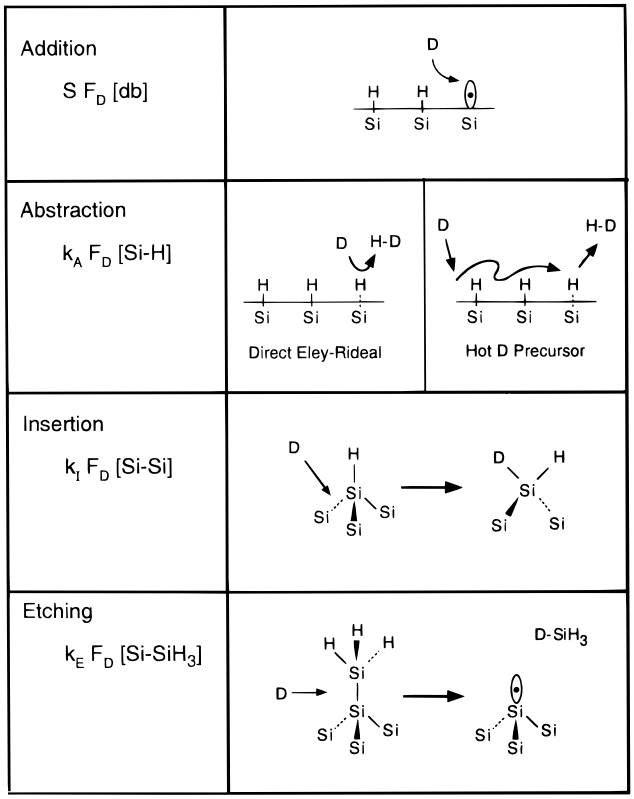

Figure 1. Schematic illustration of four principal reaction pathways for the interaction of D atoms with a silicon hydride surface: addition (sticking), abstraction, insertion, and etching. Also shown are characteristic expressions for the reaction rates of each process. See text for discussion.

(ER mechanism) for simplicity, although both ER and Langmuir−Hinshelwood (LH) mechanisms are possible for etching processes. During exposure of Si films and surfaces to H_{at}, *more than one* of these reactions can occur simultaneously.

Also shown in Figure 1 are rate expressions. Each reaction rate depends on the surface coverage or local concentration of the reacting species which are _−Si, H−Si, and Si−Si in reactions 1, 2, and 3, respectively. These reactions may have different rates in the "bulk" of a film compared to the film surface, due to differences in the rate coefficient or the local concentration (coverage). The rate coefficient of (1) is the "sticking probability", *S*, and is generally assumed to be near unity. Schulze and Henzler measured *S* on the Si(111)-(7×7) surface and obtained a value of 1, within 30%.[31] The rate of (2) is written in Figure 1 assuming a reaction with monohydride (MH) species. We write the rate of (3) as $k_I F_D\{\text{Si}-\text{Si}\}$, where {Si−Si} represents the coverage or bulk density of strained Si−Si bonds, and F_D the D atom flux. The rate coefficients k_I will be larger for strained Si−Si bonds compared to unstrained bonds. In a-Si:H films, the disorder results in a distribution (range) of Si−Si bond strengths with some weaker and some stronger, as described by Street and co-workers.[32] Weak Si−Si bonds in a-Si:H are identified with the optical absorption at energies just below the bandgap (the Urbach tail).[15] These may control the electronic properties of the a-Si:H. Another example is a "backbond" between first- and second-layer Si atoms on a reconstructed crystal Si surface.[12] Modification of a-Si:H using H_{at} preferentially removes the weakest Si−Si bonds, and our experiments are most sensitive to the most reactive Si−Si bonds (those with largest k_I).

For simplicity, we write one example rate expression for an ER etching reaction as $k_E F_D\{\text{Si}-\text{SiH}_3\}$. If there are other surface precursors to etching in addition to Si−SiH$_3$, a similar rate expression should be written for each. Reaction 2 has been previously studied on monohydride-terminated Si(100)-(2×1) and Si(111)-(7×7) by direct recoiling using thermally generated atomic H and D[9] and by other methods using hyperthermal H atoms.[11] Atomic H reactions with the disilane molecule have been investigated both experimentally[33] and using computational methods.[34] These results give information on the surface abstraction and etching reactions (see Discussion section).

II. Experimental Details

MIR-FTIR studies were performed at N.Y.U. to obtain Si−H bonding information. Kinetic studies were performed at IBM using time-of-flight (TOF) direct recoiling (DR) spectroscopy, or TOF DR, with mass separation of recoiled H^+ and D^+ ions as described previously.[9] IR characterization and kinetic results are compared for two kinds of samples. One is a thin film of polycrystalline Si prepared by growth at 200 °C on top of a crystallized seed layer, which we call "polycrystalline monohydride" (PMH). This designation is based on the IR spectrum, which resembles that of the monohydride on single-crystal surfaces (see Results section). The second sample is a film of amorphous SiH_x polymer prepared at −110 °C, which we designate "polysilane" (PS). Both films are grown in situ on top of the native oxide on a Si(100) sample or on top of Si deposited on the native oxide. Before each experiment, the sample was annealed at 600 °C, which makes a crystallized seed layer. A fresh film was then grown for each experiment. All films used here were prepared from Si_2H_6 by filament-assisted (FA) growth using a Si_2H_6 pressure of 10^{-5} Torr with a hot filament (temperature of ∼1550 °C, measured by an optical pyrometer) near the sample.

The growth flux resulting from Si_2H_6 plus the hot filament has not been characterized directly. We believe that some Si_2H_6 is decomposed on the filament, producing a stable metal silicide and H_{at} desorbing from the silicide surface. At 10^{-5} Torr pressure, the mean free path of H_{at} exceeds 100 cm, so that gas-phase reaction of H_{at} with Si_2H_6 is excluded. According to this model, the growth flux consists primarily of H_{at} impinging on intact, physisorbed Si_2H_6 molecules. For the case of FA PS growth at −110 °C, we have demonstrated that the rate of PS deposition increases with added D_2 and that the growth rate is roughly proportional to the D_2 pressure.[35] These data support the model that at least one growth mechanism at −110 °C involves D atoms initiating reaction of physisorbed Si_2H_6. At 200 °C substrate temperature (growth of the PMH film), the surface residence time of Si_2H_6 is on the order of 30 μs,[36] so this same mechanism may be active for the PMH film case. The growth mechanism will be discussed in more detail elsewhere.[35] In both chambers, D_{at} was generated by flowing D_2 through the chamber into a turbomolecular pump and dissociating the gas on a tungsten filament at ∼1550 °C. The absolute flux of D_{at} is unknown but is estimated as roughly 1% of the D_2 flux (ref 9, and references therein). The D_2 pressure was always 1×10^{-5} Torr, an ionization gauge reading, not corrected for the relative ionization probability of D_2, which is 0.42 with respect to N_2.[37]

We note the difference in sampling depth of the MIR-FTIR and TOF DR measurements. On a well-defined surface, the two methods probe the same species. In both the PMH and PS films, TOF DR probes the surface hydrides. The TOF DR signal is primarily from the first layer, with some signal from the second and third layers (due to the small incident angle of 3°). In the present MIR-FTIR experiments, *the entire thin films is probed* rather than the surface layer, and the difference between MIR-FTIR and TOF DR probe depth is most significant for the PS film.

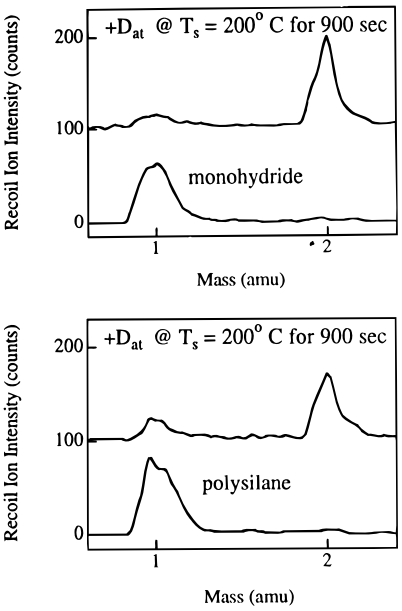

Figure 2. Top: Time-of-flight (TOF) recoiled ion data from the PMH film. Bottom: Example TOF recoiled ion data from the PS thin film.

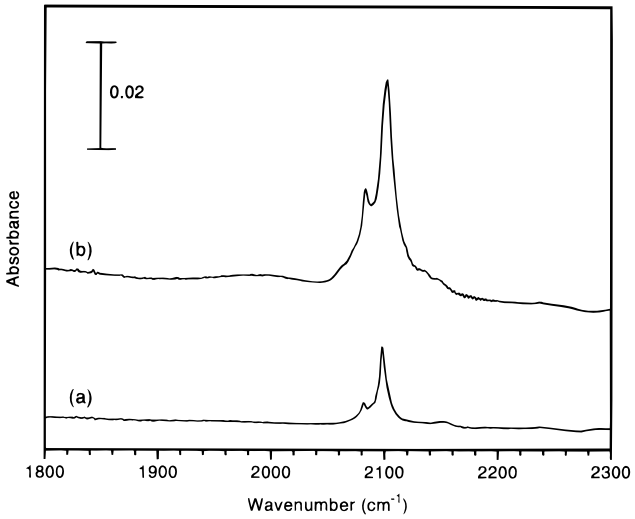

Figure 3. Infrared absorbance spectra of silicon monohydride species. Spectrum b from the polycrystalline monohydride (PMH) thin film is characterized by two peaks, a symmetric stretch at 2083 cm^{-1} and an antisymmetric stretch at 2102 cm^{-1}; the fwhm of the antisymmetric stretch mode is 15 cm^{-1}. For comparison, spectrum a is from a monolayer of monohydride species and has a fwhm of the antisymmetric stretch mode of 7 cm^{-1}.

The MIR-FTIR instrument and the data collection procedure have been described previously.[29] Some of the present experiments were performed with base pressures up to 10^{-7} Torr with no discernable effects on the data. Although both sides of the sample are probed by the IR, the PMH and PS films were grown and reacted with D atoms only on the front face. Any IR absorbance from the back face is removed by referencing to a background spectrum acquired immediately prior to growth of the film.

In the TOF DR studies, a 10 keV K^+ ion beam is pulsed at 50 kHz and impinged at a grazing incident angle (α) of 3° to the surface. Direct recoil (DR) particles are formed by a binary collision of K^+ with a surface atom. A fraction of these are recoiled ions (RI), which are mass analyzed by TOF using a "reflection" energy/time focusing electrostatic analyzer.[9] The analyzer is located at a recoil angle, Φ, of 60°, measured from the incident ion beam. The H^+ and D^+ recoil ion signals are well resolved, as shown in Figure 2. Each spectrum is signal averaged for 30 s. The K^+ beam current measured at the crystal is 0.2 nA, which in 900 s corresponds to an ion dose of ~1−2% ML. To study isotopic exchange kinetics, the PMH or PS film is exposed to D_{at}, and simultaneously TOF DR spectra are acquired and stored until a set (20−40 spectra) is complete. The *relative* coverages of H (θ_H) and D (θ_D) are determined by integrating the H^+ and D^+ ion signals (see Figure 2). Studies on well-defined surfaces show a linear relation between coverage and the H^+ or D^+ signal.[9] Here, we are analyzing thin films (not well-defined surfaces), so the coverage units are simply the H^+ or D^+ RI signals, with no absolute calibration.

III. Results

A. Polycrystalline Monohydride: Preparation and Reaction. The monohydride films were grown by heating the sample to 600 °C to crystallize the Si seed layer and then using FA CVD from Si_2H_6 for 15−30 min at 200 °C. An MIR-FTIR spectrum appears as spectrum in Figure 3, and the designation "polycrystalline monohydride" (PMH) is based on this spectrum, which shows a narrow linewidth and no features due to higher hydrides. Also shown in Figure 3 is the IR absorbance spectrum a of a monohydride-terminated silicon film grown by a different method, detailed in ref 29. Briefly, the film shown in Figure 3a was prepared by annealing a polysilane (PS) film to 600 °C and using disilane exposure (without a hot filament) during cooling from 600 °C to terminate the surface with monohydride. The resulting material was first labeled an amorphous monohydride film[29] but is more correctly described as polycrystalline. The assignment is based on comparison of the two peaks at 2098 and 2082 cm^{-1} to crystalline silicon surfaces. The peak at 2098 cm^{-1} was assigned to the symmetric stretch of dimerized monohydride species, similar to the Si(100)-(2×1):H surface, while the peak at 2082 cm^{-1} corresponds to the Si−H stretching frequency reported for the Si(111) surface.[29] Figure 3 suggests that most of the resulting surface is Si(100)-like, with a small population of Si(111) facets.[29] Recent work by Chabal and co-workers on H-implanted silicon is in agreement with this assignment.[25] The material prepared by H-implant shows an IR spectrum with similar frequencies, and transmission electron microscopy data were used to identify the (100) and (111) facets.[25] The coverage of hydrogen at the surface of the film in Figure 3a was estimated at one monolayer, in comparison with infrared and thermal desorption measurements on a Si(100)-(2×1):H surface.[29]

The spectrum from the thin film measured in Figure 3b has analogous features at 2102 and 2083 cm^{-1}, similar to spectrum 3a. This suggests that this film also contains both Si(100) and Si(111) facets and is the basis for its designation as polycrystalline monohydride, PMH. The peak width (fwhm) of the PMH film is about 15 cm^{-1}, compared to 7 cm^{-1} for the 1 ML monohydride. The integrated intensity of Figure 3b is about 4 times that of 3a, suggesting that the PMH film contains the equivalent of several monolayers of hydrogen. We do not know the absolute H content of the film, so an accurate thickness cannot be calculated from the data of Figure 3.

Figure 2 illustrates examples of the TOF DR data used to measure the relative coverage of H and D (θ_H and θ_D) in real time. The H^+ and D^+ signals are well resolved, so θ_H and θ_D can be measured from the peak areas without fitting or deconvolution. The top panel of Figure 2 is for a PMH thin film reacting with D_{at}. The lower curve was acquired from the PMH film as prepared, and the upper curve was acquired after 900 s exposure to D_{at} at 200 °C.

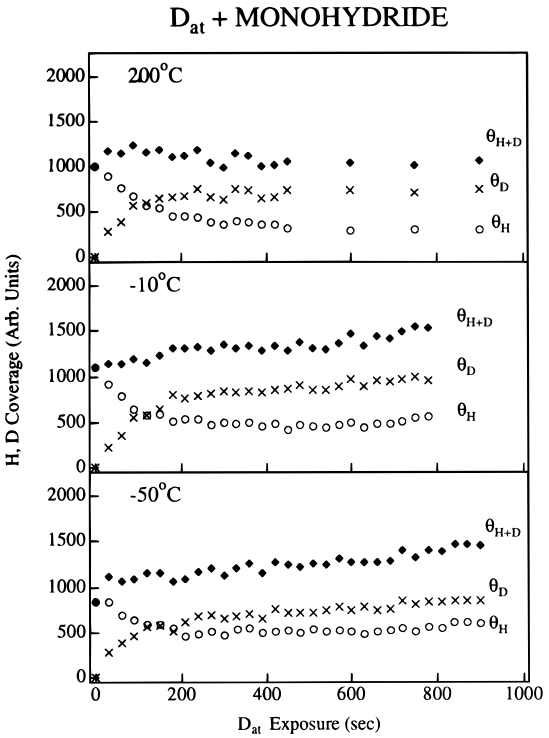

Figure 4. Surface coverage of H, D, and H+D on the PMH thin film versus D atom exposure (in seconds) measured by TOF recoiling. At zero exposure, the film is terminated only with monohydride. Reaction temperatures are 200, −10, and −50 °C.

The kinetics of isotopic exchange on the PMH thin film were studied as a function of T_S using D_{at} as the reactive atom. Summaries of selected TOF DR experiments are shown in Figure 4 for three different film temperatures. Here, θ_H (open circles), θ_D (crosses), and the sum of ($\theta_H + \theta_D$) (diamonds) are all plotted versus D_{at} exposure. Hereafter, the sum of ($\theta_H + \theta_D$) is refered to as the "total hydride coverage". Data taken at 100 and 27 °C are not shown, but are very similar to the data collected at 200 °C. At 200 °C, the total hydride coverage remains approximately constant throughout the experiment, to within ±10% (the scatter in the data). This observation is important because it implies that higher deuterated species (such as SiHD, SiD_2, or SiD_3) are unstable at 200 °C, and this is consistent with IR results on monohydride-terminated Si films, where no stable insertion products are seen at 200 °C.[29] Below room temperature the total hydride coverage increases, indicating that stable insertion products are formed. At all temperatures studied, θ_H decreases rapidly in the initial 200−500 s and then remains about constant for the duration of the exposure to D_{at}. At all temperatures, θ_D increases rapidly in the initial 200−300 s. At high T (27−200 °C), θ_D stays constant after the initial rapid increase. At lower T, a slowly changing component is seen in θ_D, from roughly 300 to 800 s. We attribute this to reaction 3 and the formation of stable insertion products, $SiHD_x$ ($x = 1, 2$). Analysis of the data of Figure 4 is discussed in section IV.

B. Polysilane: Preparation and Stability. To study the reaction of D_{at} with the di- and trihydride species, we prepared "polysilane" (PS). This polymeric material contains a mixture of tri-, di-, and monohydride species and is grown at −110 °C. Infrared spectra of a polysilane film deposited using a Si_2H_6 pressure of 1×10^{-5} Torr and the hot filament are shown as a function of deposition time in Figure 5b−d. The broad, asymmetric peak of the silicon hydride stretch has a maximum at 2120 cm^{-1} with a fwhm of 75 cm^{-1}. The frequency distribution of the SiH stretch indicates the presence of

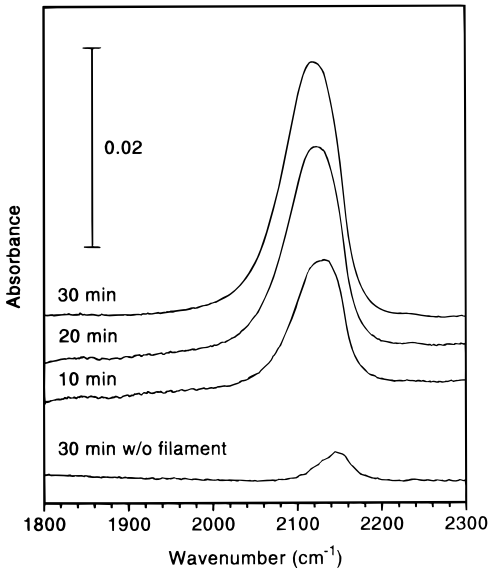

Figure 5. Infrared absorbance spectra of the silicon hydride stretching region during growth of the polysilane film. Spectra are shown after 10, 20, and 30 min of filament-assisted growth from Si_2H_6 at 1×10^{-5} Torr pressure and a sample temperature of −110 °C. Also shown is the spectrum obtained after 30 min Si_2H_6 exposure at −110 °C in the absence of a hot filament, with a peak maximum at 2150 cm^{-1}.

substantial concentration of both di- and trihydride species, as well as some monohydride.

The assignments for the silicon hydride stretching modes are as follows. Trihydride absorption occurs near 2143 cm^{-1} both in porous Si[38] and in thick a-Si:H films.[39] On single-crystal Si surfaces the SiH_3 stretch can be observed at 2154 cm^{-1}.[26,27] This SiH_3 absorption feature is evident in our infrared spectrum of disilane (Figure 5a). Silicon mono- and dihydride stretching frequencies have not been consistently assigned, as discussed by Glass et al.,[38] but occur within the range 2000−2120 cm^{-1}.[39] Some of the discrepancy in assignment can be attributed to different materials used in the various studies: single crystalline, porous, or amorphous silicon. The consensus is that the lower frequencies (2000−2090 cm^{-1}) are due to monohydride species, while the higher frequencies (2090−2120 cm^{-1}) are assigned to dihydride.[23,38−41] This assignment is consistent with our thermal annealing data (see Figure 6), where we see a shift to lower frequencies as the surface temperature is increased, in agreement with a shift to lower hydrides at higher temperatures.[29] Although the peak shape is unchanged with increasing exposure, the total integrated absorbance over the Si−H stretching region does not increase linearly with exposure time. The integrated area of the IR absorbance after 30 min of growth qualitatively suggests that the flims are 5−10 layers thick.

We compare the PS film of Figure 5 with films grown by Hirose and co-workers using a SiH_4 plasma at a similar temperature.[41,42] At −110 °C, Hirose deposited a polymer consisting primarily of polysilane chains $H_3Si-(SiH_2)_n-SiH_3$, based on the IR spectrum.[41,42] Comparison of the IR spectra of the Hirose polysilane film and the present PS reveals that our filament-assisted process results in higher concentrations of isolated monohydride species. We also compare the data at the top of Figure 5 with IR spectra resulting from Si_2H_6 exposure at −110 °C in the absence of a hot filament. The IR spectrum shown at the bottom of Figure 5 is assigned to disilane multilayers. The peak position is shifted to 2150 wavenumbers, characteristic of SiH_3 species, and is much less intense than that produced in the presence of the hot filament. At still lower temperatures (∼−173 °C), thick films of disilane could be

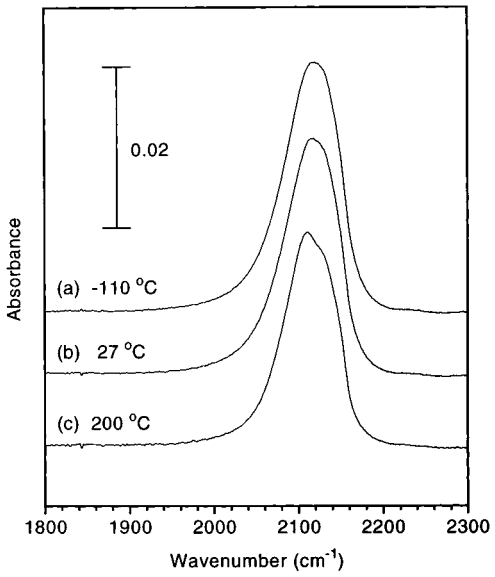

Figure 6. Thermal stability of polysilane films as measured by infrared absorbance of the silicon hydride stretching region. The top spectrum is of a polysilane film deposited after 30 min at −110 °C. Lower traces show absorbance spectra after annealing to 27 and 200 °C for 1 min. Annealing at 200 °C for 30 min resulted in no further change in the spectrum.

adsorbed, with the spectra showing fundamental and overtone modes in close agreement with solid Si_2H_6 spectra.[43]

Thermal stability of the present PS films is examined spectroscopically in Figure 6. Data from the PS film as grown appears as Figure 6a. IR spectra recorded after annealing the film to 29 and 200 °C appear as Figure 6b,c, respectively. Comparing spectra 6a and 6b results in a 15−20% decrease in integrated absorbance intensity, and the same decrease is observed after 1 min and 30 min (the duration of the kinetics experiments presented below) at 200 °C. Accompanying the small intensity decrease is a change in the peak shape, with a slight decrease of the higher frequency components. The data of Figure 6 indicate that the PS films are stable to at least 200 °C in the absence of D_{at} or H_{at}.

C. Polysilane: Reaction with D Atoms. The reactions of PS films with D_{at} were studied at surface temperatures ranging from 200 to −110 °C. Loss of surface H and increase of surface D were followed both by MIR-FTIR and by TOF DR. As discussed in the Experimental Datails section, the IR measurements probe throughout the thin film, while TOF DR is sensitive only to the film surface. Infrared spectra are shown in Figure 7 of a polysilane film as deposited (7a) and after D_{at} exposure at −110 °C (7b). Also shown is the IR spectrum after exposure at 200 °C (7c). Approximately 90% of the SiH_x groups are removed after 15 min of D_{at} exposure at 200 °C, corresponding to a loss of several layers of material (assuming a film thickness of 5−10 layers). At 200 °C, the silicon deuteride that is formed after reaction of PS with D_{at} is characterized by a relatively sharp peak (fwhm = 22 cm^{-1}) at a frequency of 1530 cm^{-1} (Figure 7c and inset). This spectrum is assigned to a monodeuteride by comparison with monodeuteride-terminated Si(100), which exhibits a strong symmetric stretching mode at 1530 cm^{-1} and a weaker asymmetric stretch at 1519 cm^{-1}.[24,44] The IR data indicate that at 200 °C existing mono-, di-, and trihydride species are removed throughout much of the film and are replaced primarily by monodeuteride.

At −110 °C, removal of H atoms in the PS film by D atoms is less complete. The spectrum in Figure 7b for PS after 30 min of D_{at} exposure at −110 °C shows only a 30% decrease in the integrated Si−H peak area. Concurrent with the loss of

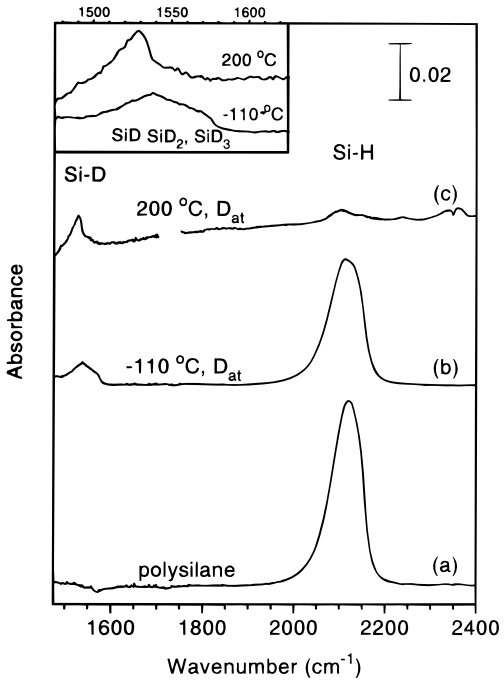

Figure 7. Infrared spectra of a polysilane film as deposited (a) and after D atom exposure at −110 °C (b) and at 200 °C (c). The inset shows the Si−D stretching region from b and c with an expanded scale indicating the stable products of insertion of D_{at} into Si−Si bonds.

hydrogen, a small, broad peak centered at 1541 cm^{-1} appears, as shown in the inset to Figure 7. This absorbance is characteristic of a distribution of higher silicon deuterides (SiD_2 and SiD_3 groups). On crystalline Si, the dideuteride exhibits a strong absorption at the asymmetric stretching frequency of 1541 cm^{-1}. The symmetric stretch at 1516 cm^{-1} is much weaker.[24] The stretching frequencies for SiD_2 and SiD_3 in amorphous and porous Si appear at higher wavenumbers compared to the monodeuteride.[38,44]

Polysilane films were studied by TOF-DR during exposure to D_{at}. The bottom panel of Figure 2 illustrates TOF-DR spectra before and after exposure of PS to D_{at}. It is useful to compare the bottom and top panels of Figure 2. After equivalent D_{at} exposures θ_H is larger for the PS film than for the PMH film. This could be due to slower reaction rates on polysilane or due to transport of H to the surface from the subsurface layers of the PS film (see Discussion section).

Figure 8 summarizes the polysilane results at different temperatures. Signals for θ_D (crosses), θ_H (circles), and total hydride coverage (diamonds) are all plotted. Figure 8 can be compared with the results for the PMH film in Figure 4. Similarities are seen. For example, below room temperature the total hydride coverage *increases* for both the PS (Figure 8) and PMH (Figure 4) thin films at similar rates. There are two differences in the PS isotopic exchange kinetics, compared to PMH. At 200 °C, the total hydride signal *decreases* in the PS case, an effect we attribute to etching, reaction 4. A similar decrease occurs at 100 °C (not shown), but not below 100 °C. The second difference between the two types of thin film can be seen near zero time. The period of the initial drop in θ_H and rise in θ_D near zero time lasts longer (300−430 s) in the PS case compared to PMH. Evaluation of rate constants from these data is discussed in section IV.

IV. Analysis of Kinetic Data

The isotopic exchange experiments (Figures 4 and 8) were analyzed to evaluate reaction rates. In Figures 4 and 8, both

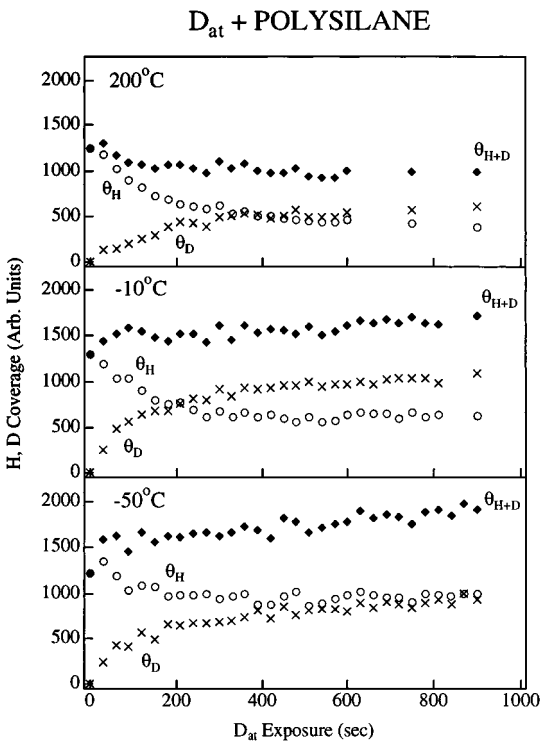

Figure 8. Surface coverage of H, D, and H+D measured on the polysilane film versus D atom exposure (in seconds) by TOF recoiling. At zero exposure, the film contains only hydride species. Reaction temperatures are 200, −10, and −50 °C.

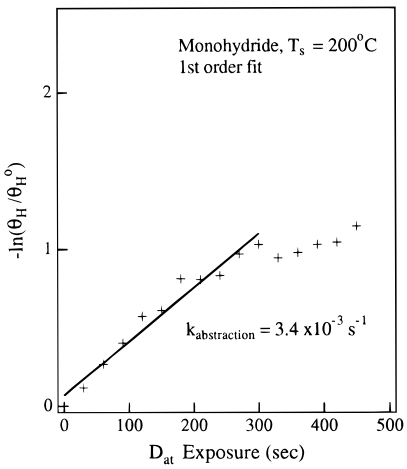

Figure 9. H coverage data from the top panel of Figure 4 for the PMH film plotted versus D atom exposure (in seconds), using a first-order rate analysis. The solid line shows the least-squares fit from 0 to 300 s, with the abstraction rate coefficient given by the slope.

θ_H and θ_D exhibit rapid changes in the first 200−300 s of D_{at} exposure, followed by a slow component at longer times. In section A, we consider only the change in the hydrogen coverage; changes in the deuterium atom coverage are treated in section B.

A. Transients in Hydrogen Coverage, θ_H. A decrease in θ_H in the presence of a D atom flux can occur by abstraction, reaction 2, or by etching, reaction 4. We consider reaction with the PMH film first. In Figure 9, we replot the θ_H data set from the top panel of Figure 4 (200 °C) for the PMH thin film according to a first-order rate expression. The fit to first-order kinetics is acceptable over the first 300 s and yields a rate constant for abstraction of 3.4×10^{-3} s^{-1}. A slightly higher rate coefficient (4.4×10^{-3} s^{-1}) is obtained by fitting only the first 200 s. After 200−300 s, the data no longer fit a single first-order rate expression. Using an estimate of the equivalent D_{at} flux for the first 300 s as 0.1 langmuir/s, we calculate that surface hydrogen depletion occurs after exposures of 20−30 langmuirs of D_{at}.

On the basis of the following analysis, we assign the fast component of the PMH film data to an abstraction reaction alone. According to the infrared spectrum (Figure 3), the PMH film contains only monohydride species. By examination of Figure 9, we conclude that a mechanism to remove H and replace it with D is active on a film containing *only monohydride species* and that this mechanism is active as soon as the D_{at} exposure begins. Specifically, there is no evidence for an induction period. If hydrogen was removed by surface etching, the resulting rate would show an induction period because an etching mechanism (for example, reaction 3 followed by 4) requires surface trihydride species. Therefore, an etching reaction would be expected to exhibit a dependence on the {Si−$SiHD_2$} coverage, and the rate of such a mechanism would depend on the D_{at} exposure. The etching rate should be zero near zero D_{at} exposure, when only Si−H species are present. Then, the coverage of {Si−$SiHD_2$} must increase during the D_{at} exposure, for example by the insertion mechanism discussed below, leading to an increase in the etching rate. Such a mechanism would lead to an induction period to etching, but the data are inconsistent with this model of hydrogen loss.

Other evidence for abstraction alone was obtained in an earlier IR study of monohydride reactions.[29] After exposure to D_{at} at 200 °C, the IR spectra showed no stable insertion products,[29] indicating that the rate of etching (reaction 4) or other related reactions) is much slower than abstraction at 200 °C, because stable trihydride species are absent.[29] Abstraction (reaction 2) is known to be rapid on monohydride species on crystal Si.[9−11] We believe etching is negligible for this surface, and the initial rapid decrease in θ_H is due to abstraction.

First-order rate coefficients for reaction 2 from the PMH thin film were calculated from plots similar to Figure 9, obtained for TOF-DR experiments at various temperatures. These rate coefficients are listed in Table 1, along with the correlation coefficients for each fit. The quality of the fits is good for temperatures $\cong$ −50 °C, implying that the initial reaction is first order over the temperature range −50 to 200 °C. The rate coefficients for reaction 2 measured on the PMH thin film are similar in magnitude to the same data for the pure monohydride phase on the Si(111) and the Si(100) single-crystal surfaces.[9]

Isotopic exchange experiments using TOF-DR were conducted on the polysilane films at the same temperatures. The TOF-DR data from PS at 200 °C (top panel of Figure 8) are plotted according to a first-order rate expression in Figure 10. Data for the first-order rate coefficient and the respective correlation coefficients are given in Table 1 for several surface temperatures. As for the PMH film data, the quality of the fit varies with temperature. In the PS case the fit to the first-order rate expression over the first 300 s is acceptable, and the correlation coefficient is similar to that for the PMH film at 200 °C (Table 1).

Etching plays a role in the rate of hydrogen loss for the polysilane film. Because the PS film contains trihydride species (determined by analysis of the infrared spectrum, Figure 6), etching reactions such as (4) are facilitated. Also, the infrared data of Figure 7 obtained at 200 °C clearly show that several layers of silicon hydride are removed by D_{at} exposure, indicating that etching is an active reaction pathway at this temperature. Another complicating factor affecting the rate of change in θ_H with time for polysilane at 200 °C could be transport (diffusion) of H to the surface layer from the "bulk" of the thin PS film

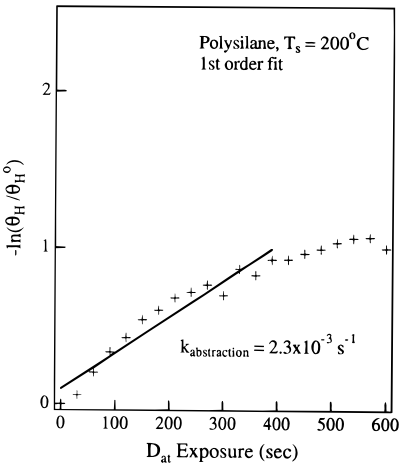

Figure 10. H coverage data from the top panel of Figure 8 for polysilane plotted versus D atom exposure (in seconds), using a first-order rate analysis. The solid line shows the least-squares fit from 0 to 300 s, with the abstraction rate coefficient given by the slope.

TABLE 1: First-Order Kinetic Analysis Using θ_H: PMH = Polycrystalline Monohydride, PS = Polysilane, C.C. = Correlation Coefficient

T_s (°C)	T_s (K)	$1/T_s \times 1000$	k(PMH)	C.C.	k(PS)	C.C.
200	473	2.11	3.4×10^{-3}	0.982	2.3×10^{-3}	0.963
100	373	2.68	4.7×10^{-3}	0.981	3.6×10^{-3}	0.973
−10	263	3.80	4.2×10^{-3}	0.968	3.1×10^{-3}	0.990
−50	223	4.84	2.3×10^{-3}	0.982	1.2×10^{-3}	0.880

(see Discussion section). Etching removes H from the PS surface region, while transport would add to the H in this region. Due to these two competing reactions, the first-order rate coefficients for reaction of D_{at} with PS reported in Table 1 must be viewed as *estimates* of the abstraction rate from PS.

B. Transients in θ_D at Longer Times. The hydrogen coverage is directly affected only by reactions 2 and 4, but the deuterium coverage at the surface may potentially be influenced by all four reactions shown in Figure 1. Addition and insertion cause an increase in θ_D, while abstraction and etching contribute toward a loss of θ_D. To identify the dominant mechanisms, we refer again to Figure 4 and to Figure 8. For D_{at} exposure at −10 and −50 °C the change in θ_D has two components: a fast rise at short time followed by a slow component at longer times (>300 s). We have plotted the change in θ_D according to a first-order rate analysis for both the PMH and PS films at T_S = −10 °C in Figure 11, where the "slow" and "fast" components are easily distinguished.

The rapid θ_D increase near zero time (the fast component in Figure 11) is assigned to addition (reaction 1), occurring on dangling bond sites created by abstraction (reaction 2). Insertion (reaction 3) must also be considered, but IR shows no evidence for stable di- or trihydride species following D_{at} exposure at 200 °C.[29] Only monodeuteride is stable at 200 °C (see Figure 7, top). Also, the data of Figure 4 show no net increase in total hydrogen plus deuterium coverage at 200 °C, consistent with replacement of silicon monohydride with silicon monodeuteride. We believe the *rapid* transient in θ_D is not influenced by the insertion reaction.

For the "slow" component occurring from roughly 270 to 800 s, the fit to first-order kinetics is good and yields the same rate coefficient for both the PMH and PS films. The data of Figure 11 were also plotted according to a second-order rate expression, and a poor fit was obtained (not shown), so the reaction does not follow second-order kinetics. The fast component is then due to reaction 1, and isotopic exchange due to abstraction is complete after 270−300 s (evident by the hydrogen data in Figures 4 and 9). Subsequent abstraction and addition events should not significantly perturb the deuterium coverage at longer times (although these continue to occur at a rapid rate). The slow component of the θ_D signal should be independent of the addition and abstraction rates. Using the change in θ_D, we expect to minimize the influence of etching reactions in the kinetics. As discussed in section IV.A, we determine that etching can be neglected entirely in the case of the PMH film. Thus, we assign the first-order rate constants from Figure 11 to insertion, reaction 3. Comparing with the data in Table 1, this rate is about 10 times slower than abstraction for the temperature of −10 °C. At −50 °C, a very similar value of the insertion rate coefficient is obtained, 4.1×10^{-4} s^{-1} (data not shown).

V. Discussion

A. Film Preparation and Thermal Decomposition of SiH_3 and SiH_2 Species. First, we consider SiH_2 and SiH_3 decomposition in thin Si films by *thermally activated* reaction pathways. Later, we discuss reactions of atomic H with the hydride species in these films. The MIR-FTIR method has revealed many details of SiH_x chemistry on crystal Si surfaces[23−28] and in thin a-Si:H and polysilane films.[29,41,42] Porous Si with high surface area is used for transmission IR studies of Si hydrides, including measurements of the decomposition kinetics of SiH_3[38] and SiH_2.[46] Here, we have used MIR-FTIR not as a surface probe but as a method of probing an entire thin film by transmission IR. As shown previously by Hirose,[41,42] the sensitivity of MIR-FTIR allows us to study the preparation and thermal stability of amorphous Si films with a thickness of a few MLs. Filament-assisted CVD (FA CVD) from Si_2H_6 is convenient for film preparation in situ in high vacuum or UHV.

When a growth temperature of 200 °C is used, it is clear from the data of Figure 3 that FA CVD from Si_2H_6 produces a film terminated with monohydride species. By comparison with the stretching frequencies and line widths of Si−H on crystal Si surfaces[24] and in Si samples implanted with H,[25] we conclude that the spectra in Figure 3 indicate a crystalline film, as discussed in section III (Results). We do not know the grain size of this film, so we have used the general term polycrystalline, calling the film "polycrystalline monohydride" or PMH. Microcrystalline may be a more accurate description, but we use the more general term. Figure 3 illustrates the in situ growth of a Si thin film terminated with only monohydride. This is one model system to study the reactions occurring during PE CVD growth and "chemical annealing" of a-Si:H.

Reaction rate data for SiH_3 and SiH_2 species will help us to eliminate these groups from a-Si:H films when the films are grown at 30−200 °C (low-T growth). When cryogenic growth temperatures are used, FA CVD from Si_2H_6 (see Figure 5) produces a film containing abundant SiH_2 and SiH_3 species, which we call polysilane (PS). The MIR-FTIR data of Figure 5 confirm that the presence of a hot filament is required for growth of PS films. This film is similar in some respects to the PS made by Hirose and co-workers.[41,42] In other respects, the FA CVD and the Hirose PS films are different. Hirose deposited PS over a range of cryogenic growth temperatures using a SiH_4 plasma. Our growth temperature of −110 °C was selected based on the Hirose studies.[41,42] At −110 °C, the SiH_4 plasma growth resulted in little or no Si−H and some SiH_3, and the major component of the film was dihydride in the form of $(SiH_2)_n$ chains with n of order 10.[41]

The broad features seen in Figures 5 and 6 indicate that the PS prepared here by FA CVD at −110 °C contains mono-, di-, and trihydride species. The Si−H concentration in PS is small

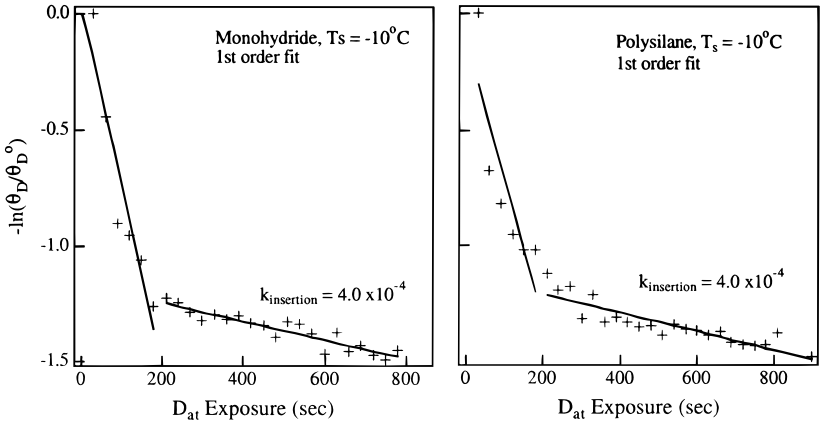

Figure 11. D coverage data from Figure 4 (PMH film) and Figure 8 (PS) at a reaction temperature of −10 °C for both films plotted versus D atom exposure (in seconds), using a first-order rate analysis. The solid lines show least-squares fits to different sections of the data, with the insertion rate coefficient given by the slope of the slow component.

compared to that of the di- and trihydride, as seen in spectra 6a and 6b. The line shape from our FA CVD PS is distinctly broader than that from Hirose's PS,[41,42] due to the presence of Si−H species. If we make the simple approximation that the oscillator strengths of the three hydride species are the same, Figure 5 suggests that SiH_2 is the major component, with somewhat less SiH_3 and Si−H present in the PS as prepared at −110 °C. As discussed in section III, we assign the lower frequencies (2000−2090 cm^{-1}) to monohydride species and the higher frequencies (2090−2120 cm^{-1}) to dihydride.[23,35−39] The trihydride stretching frequency is at 2148 cm^{-1}, or slightly higher depending on the material. Both in porous Si[38] and in thick films of a-Si:H,[36] the SiH_3 stretch is seen at 2148 cm^{-1}. On the Si(111)-(7×7) surface, SiH_3 prepared by low-temperature chemisorption of Si_2H_6 exhibits the Si−H stretch at 2154 cm^{-1}.[26,27]

The thermal stability of the PS made by FA CVD is considered (Figure 6) by comparing spectrum 6b with 6a. Annealing PS at room temperature has very little effect on the distribution of hydride species. In the form of PS, the di- and trihydride species are stable at room temperature. In thick a-Si:H films grown near 100 °C, these species are readily detected by IR.[39] In contrast, on crystal Si surfaces SiH_3 decomposition can be observed well below room temperature, as seen by IR spectroscopy on the Si(111)-(7×7) surface[26,27] and temperature-programmed secondary ion mass spectrometry on Si(100).[47] We conclude that *decomposition rates of SiH_3 by thermally activated routes depend on the local environment surrounding the SiH_3 groups*.

One mechanism of SiH_3 decomposition is reaction with a nearby dangling bond, reaction 4.

$$SiH_3 + \_ \rightarrow Si{-}H + SiH_2 \qquad (4)$$

A very different mechanism of SiH_3 decomposition is disproportionation (reaction with itself). Recently, Glass, Wovchko, and Yates (GWY) used IR transmission through electrochemically prepared porous Si samples to study SiH_3 decomposition.[38] GWY increased the SiH_3 population through H_{at} exposure and then observed *complete SiH_3 decomposition* in the range −148 to −60 °C. This decomposition is thought to occur by a disproportionation reaction 5.[38]

$$2SiH_3 \rightarrow SiH_4(g) + SiH_2 \qquad (5)$$

A related reaction (6) with SiH_2 may also occur, but SiH_3 is the most reactive of the three hydrides.

$$SiH_3 + SiH_2 \rightarrow SiH_4(g) + SiH \qquad (6)$$

Most of the SiH_3 species present in our PS film as prepared (Figure 6a) are isolated from each other, so that reaction 5 cannot occur at a significant rate. It follows that the SiH_3 are also isolated from dangling bonds and SiH_2 species. Reactions 4−6 can be rapid even at cryogenic temperatures when the coreactant (either a dangling bond, _, a second SiH_3 group, or SiH_2) is present in high concentration. When SiH_3 is isolated from coreactants, it is stable at room temperature (see Figure 6). When the PS film is annealed at 200 °C, the population changes by decomposition of SiH_3 species, leaving SiH_2 as the dominant hydride. See spectrum 6c. Some SiH_3 species remain even after 200 °C annealing, and these must be isolated minority species in a network containing mainly SiH_2 and Si−H groups.

Terminology from surface chemistry identifies reactions 5 and 6 as second order, Langmuir−Hinshelwood (LH), etching processes. Figure 7 of this work suggests that the etching rate of PS by D_{at} has a strong surface temperature dependence, and this is consistent with an LH, surface-mediated, second-order mechanism. The GWY study demonstrated decomposition of SiH_3 with a rate that is strongly temperature dependent. This is characteristic of the LH mechanism.

B. Nonthermal Decomposition of Hydride Species. Decomposition of SiH_3 by *thermally activated* pathways (subsection A) is a baseline for probing the "chemical annealing" effect.[19−22] Now, we distinguish thermal pathways from decomposition pathways that are *activated by an H_{at} flux*. The latter are expected to fall into two categories: reaction pathways that directly involve H_{at} as a reactant (such as the etching process shown in Figure 1 and reaction 7 below) and pathways with H_{at} acting *indirectly* by creating dangling bonds near an SiH_2 or SiH_3 species. (The local environment near an SiH_2 or SiH_3 species could be perturbed in other ways by H_{at}, but dangling bond creation is the important concept in the indirect action of H_{at} to decompose the higher hydrides.) The dangling bonds may facilitate diffusion or may speed decomposition by reactions such as (4). Reactions of the first type should have a first-order dependence on the H_{at} flux. In the second case, H_{at} may increase the rate of surface decomposition of the higher species, but H_{at} does not appear explicitly in the elementary rate expression for decomposition. It may be impossible or very difficult to obtain solid evidence for reactions with H_{at} acting indirectly.

Reactions 7 and 8 are examples of Eley−Rideal (ER) etching processes with a first-order dependence on the H_{at} flux. Reaction 8 was proposed by Jasinski based on mass spectrom-

etry of silicon hydride species formed by exposure of a-Si:H to H_{at}.[48] Reaction 8 is direct formation of gas-phase silyl via a surface reaction, while reaction 7 is formation of SiH_4. Computational studies using the Si_2H_6 molecule as a model system suggest the barriers are small for both reactions 7 and 8.[34]

$$H_{at} + Si{-}SiH_3 \rightarrow SiH_4(g) + Si{-} \quad (7)$$

$$H_{at} + Si{-}SiH_3 \rightarrow SiH_3(g) + Si{-}H \quad (8)$$

Figure 7 demonstrates that PS is etched by H_{at} exposure rapidly at 200 °C and very slowly at −110 °C. The temperature dependence seen in Figure 7 suggests that LH mechanisms (such as reactions 5 and 6) are active when PS is exposed to H_{at}. Reactions involving ER mechanisms such as (7) and (8) may occur in parallel with LH mechanisms. The data suggest that LH mechanisms may play a role during etching and "chemical annealing" with H_{at}.

C. Kinetics of Abstraction, Reaction 2. Whenever a Si film or surface containing hydride species is exposed to H_{at}, abstraction occurs (reaction 2). This is the most rapid reaction of H_{at} with *Si−H bonds*. Only adsorption at dangling bonds, reaction 1, is more rapid. The rate of reaction 2 with monohydride species has been followed in real time on both Si(100) and Si(111) surfaces.[9] These studies emphasized surfaces terminated with 1 ML of Si−H prepared at 505 °C, but fractional ML coverages were also studied. It was shown that the rate of (2) is ∼1/3 that of (1), is independent of Si−H coverage, and is first order in D_{at} flux (F_D).[9] From the surface temperature dependence, a small activation energy (E_a) (≈0.5−1 kcal/mole) was measured. One explanation for this E_a is an enhanced rate of reaction 2 from $v = 1$ vibrational modes of Si−H, compared to $v = 0$.[9] Reaction 2 has also been observed by Weinberg and co-workers,[10] by Buntin,[11] and by Naitoh and co-workers.[49] Direct observation of (2) on a-Si:H films was reported by Abelson in 1990[50] and investigated further by Katiyar, Yang, and Abelson using IR spectroscopy.[51]

Recently, Parsons and co-workers compared the heats of reaction and barriers to abstraction from Si−H and SiH_2 species using *ab initio* calculations.[52] Small clusters of Si terminated with H were used. Abstraction from Si−H was found to be slightly more exothermic than abstraction from SiH_2, and a slightly lower barrier to abstraction was found for the monohydride.[52] A faster reaction of H_{at} with Si−H than with SiH_2 is implied.

In Table 1 we have summarized our present results for the rate coefficient of reaction 2 with the PMH film. As discussed in section IV, the first-order plots at 200 °C (Figure 9) and 100 °C show a *Y*-intercept at zero, indicating no induction ("incubation") period before H is lost from the film at a constant rate. Thus, in Table 1 the data from the PMH thin film (dots) can be readily interpreted as a measure of the rate of reaction 2, and these agree in magnitude with the corresponding rates on crystal Si surfaces.[9] We tentatively conclude that the rate of reaction 2 with *monohydride* species is not strongly dependent on the local Si−Si bonding and other structure surrounding the Si−Si group. This observation can be readily understood if two conditions are met. First, the monohydride Si−H bond strength does not change, and second the energy of the Si− dangling bond product does not change, as the nearby Si−Si bonding in the film is altered. Experimental bond dissociation energies for monohydride Si−H in films or on surfaces have not been measured directly, but were estimated by George and co-workers.[46,53] The monohydride[53] and dihydride[46] bond energies were estimated to differ by 8 kcal/mole, or roughly 10%. Another experimental point of comparison is measured Si−H bond dissociation energies in SiH_4 and Si_2H_6.[54] Substituting one Si−Si bond for one Si−H bond changes the remaining Si−H bond energy by about 5%.[54]

Due to the other reactions that compete with abstraction, our conclusions in the case of PS are qualitative and tentative. We believe that etching and abstraction are competing reactions that both remove H from the PS surface region. Figure 7 proves that etching is active at 200 °C and is thermally activated, although we do not have isothermal rate data for etching. The barriers for both the etching and abstraction reactions have been estimated to be small and similar in magnitude by Dobbs and Doren,[34] consistent with competing reactions. When the concentration of etching precursors ($Si{-}SiH_3$) is high, as in the PS film, the etching rate may be competitive with the abstraction rate.

Also in Table 1 are first-order rate coefficients measured from the PS film. At every temperature, the abstraction rate coefficient for reaction 2 appears consistently slower on the PS film, which is rich in di- and trihydride species, compared to the PMH thin film. This is consistent with the conclusions of the study of Parsons and co-workers,[52] in which a faster reaction of H_{at} with Si−H than with SiH_2 was predicted. Previous experimental studies indicate that isotopic exchange is slower when higher hydrides are present on Si(100) compared to the pure monohydride phase.[9,49] At 200 °C, it is possible that H is transported from within the PS thin film to replenish the surface H removed by reaction 2, which would reduce the apparent rate of H loss from PS. Such an effect should exhibit a strong temperature dependence if electronic quality a-Si:H can be used as a guide. Diffusion of H in a-Si:H has an activation energy of about 1.5 eV,[31,45] is extremely slow below 100 °C,[45] but becomes rapid at 200 °C or higher.[31,45,55] Gallagher and co-workers addressed the rate of diffusion of H in a-Si:H films at 248 °C, suggesting H atoms can diffuse a distance of four atomic layers in 100 s at 248 °C.[55] The rate of diffusion of H in PS is not known and will depend on the density of dangling bonds. The a-Si:H results suggest that H diffusion could only affect our H/D exchange experiment at 200 °C. So the systematic differences in abstraction rate coefficients at all temperatures (Table 1) are not consistent with a contribution from H diffusion.

The rate of abstraction may invovle accommodation of H_{at} (D_{at}) into a mobile precursor state weakly interacting with the film surface and intermediate between the homogeneous and chemisorbed phases.[10,56] Recently, Weinberg and co-workers studied D_{at} adsorption and pairing of D on Si dimers at −125 and 325 °C on Si(100)-(2×1).[10] They proposed that addition of H_{at} (D_{at}) and abstraction are mediated by a "hot" precursor state. Differences in surface structure between crystal Si, the PMH film, and PS may change the surface mobility of a "hot" H_{at} or D_{at} precursor, affecting the rate of abstraction.

D. Insertion of D_{at} into Si−Si Bonds. Reaction 3, insertion, is required for formation of dihydride species in films containing only monohydride and crystalline Si surfaces. A similar reaction of D_{at} with the dihydride leads to SiH_3. Insertion into Si−Si bonds is part of the chemistry of etching by H_{at} or D_{at} (see Figure 7 and refs 12, 30). Near zero H coverage, the slope of a plot of θ_H versus H_{at} exposure approximates the rate of reaction 1. Using a Si(100) surface and comparing the slopes observed in the low and high H_{at} exposure regions, the rate of (3) can be estimated as occurring at about one-tenth the rate of (1) on Si(100)-(2×1).[30] Using real-time spectroscopic ellipsometry and a-Si:H films, the bulk rate of reaction 3 has been measured at 253 °C.[21] The bulk rate coefficient, $\sim 10^{-3}$ s^{-1},[21] is very similar

to our value of 4×10^{-4} s^{-1} from Figure 11 for the surface rate of (3).

Here, we have studied the insertion reaction into the Si−Si bonds in Si films at −10 °C by exposing these films to D_{at} and following D uptake. In Figure 11, we see that the change in θ_D has both a "fast" and a "slow" component, when either the PMH or PS films are exposed to D_{at} at −10 °C. The slow component seen at large D_{at} exposures is assigned to reaction 3. Shown in Figure 11 is the rate of insertion, which is about one-tenth the rate of abstraction. In Figure 1, we write the rate of (3) as $k_I F_D\{Si-Si\}$, using {Si−Si} to mean the coverage of *strained Si−Si bonds*. As emphasized by Boland for crystal Si surfaces[12] and by Street for a-Si:H,[31] strained (weak) Si−Si bonds are susceptible to attack by atomic H or D, so relaxation of strained (weak) Si−Si bonds is one factor determining the rate of (3). The comparison made in Figure 11 indicates no detectable difference in reactivity between the Si−Si bonds in the PMH and PS films.

Two observations reported here may be influenced by diffusion or decomposition of SiH_3 species. These relate to the "chemical annealing" effect. These are (1) the absence of stable insertion products seen by IR at 200 °C and (2) the absence of a "slow" component in the θ_D measurements above room temperature. The "slow" component in our first-order plots (Figure 11) was well resolved and linear only at −10 and −53 °C and was not seen at 200 or 100 °C.

We invoke diffusion of SiH_3 species near the surface of the amorphous film to explain these observations. We suggest that insertion products (higher hydrides) are formed during D_{at} exposure at all temperatures. However, with a flux of H_{at} (D_{at}) impinging on the film, the di- and trihydride species decompose during the atom exposure above room temperature and are stable and detectable below room temperature. The stability of these species below room temperature is attributed to their immobility. Above room temperature, diffusion of SiH_3 prior to reaction 4, 5, or 6 may all be active decomposition pathways. A key role of the D atom flux may be to create dangling bonds, via reaction 2, and these dangling bonds then accelerate decomposition of SiH_3 by reaction 4. The apparent temperature dependence of the stability of bonded SiH_3 could thus be influenced by the diffusion rate of mobile SiH_3 species prior to reaction 4. Surface diffusion of the relatively unreactive silyl radical, SiH_3, during growth of a-Si:H from a SiH_4 plasma is widely invoked to explain experimental data on film conformality.[1,57] Diffusion of SiH_3 prior to reaction 4, 5, or 6 may account for the temperature dependence we see for detection of stable insertion products by IR in Figure 7 and ref 29 and for observation of insertion by TOF-DR in Figure 8.

VI. Summary

We can summarize the observations made in this work with four basic statements.

1. Polycrystalline or polymeric Si hydride films can be conveniently grown in a turbomolecular-pumped UHV system by filament-assisted chemical vapor deposition from Si_2H_6. The growth temperature can be used to change the hydride species present in the film.

2. On the PMH thin film between −53 and 200 °C, a reaction removing H and replacing it with D occurs with a rate coefficient of about $(4 \pm 1) \times 10^{-3}$ s^{-1}. The rate coefficient does not change over the D_{at} exposure range from 0 to 20 langmuirs, while the measured H coverage changes by a factor of 2. We assign this to abstraction, reaction 2. At 100−200 °C, the rate coefficient is similar to that measured for Si−H species on crystal Si surfaces.[9]

3. We have measured the rate of insertion, reaction 3. At −10 and −53 °C, the insertion rate coefficient is $\sim 4 \times 10^{-4}$ s^{-1} on both the PMH and PS thin films, about one-tenth the abstraction rate. This compares well with an earlier measure of this rate coefficient, 10^{-3} s^{-1}.[21]

4. Using a polymeric silicon hydride film, a strong temperature dependence of the rate of film etching by D_{at} has been observed. This indicates an activated etching mechanism.

Acknowledgment. S.F.B. gratefully acknowledges financial support for this work from a National Science Foundation CAREER award (Grant No. DMR-9501774) and from the donors of the Petroleum Research Fund, administered by the American Chemical Society.

References and Notes

(1) Abelson, J. R. *Appl. Phys. A* **1993**, *56*, 493.
(2) Matsuda, A.; Hata, N. In *Glow Discharge Hydrogenated Amorphous Silicon*; Tanaka, K., Ed.; Kluwer: Boston, 1989; Chapter 2.
(3) Montgomery, J. S.; Schneider, T. P.; Carter, R. J.; Barnak, J. P.; Chen, Y. L.; Hauser, J. R.; Nemanich, R. J. *Appl. Phys. Lett.* **1995**, *67*, 2194.
(4) Crossley, A.; Sofield, C. J.; Sugden, S.; Clampitt, R.; Bradley, C. *Vacuum* **1995**, *46*, 667.
(5) Shibata, T.; Nanishi, Y.; Fujimoto, M. *Jpn. J. Appl. Phys.* **1990**, *29*, L1181.
(6) Rettner, C. T. *Phys. Rev. Lett.* **1992**, *69*, 383.
(7) Hall, R.; Cadez, I.; Landau, M.; Pichou, F.; Schermann, C. *Phys. Rev. Lett.* **1988**, *60*, 337.
(8) Eenshuistra, P. J.; Bonnie, J. H. M.; Los, J.; Hopman, H. J. *Phys. Rev. Lett.* **1988**, *60*, 341.
(9) Koleske, D. D.; Gates, S. M.; Jackson, B. *J. Chem. Phys.* **1994**, *101*, 3301.
(10) Widdra, W.; Yi, S. I.; Maboudian, R.; Brigg, G. A. D.; Weinberg, W. H. *Phys. Rev. Lett.* **1995**, *74*, 2074.
(11) Buntin, S. *J. Chem. Phys.* **1996**, *105*, 2066.
(12) Boland, J. J. *Adv. Phys.* **1993**, *42*, 129.
(13) Nachtigall, P.; Jordan, K.; Sosa, C. *J. Phys. Chem.* **1993**, *97*, 11666.
(14) Sinniah, K.; Sherman, M. G.; Lewis, L. B.; Weinberg, W. H.; Yates, J. T.; Janda, J. C. *J. Chem. Phys.* **1990**, *92*, 5700.
(15) Yamasaki, S. In *Glow Discharge Hydrogenated Amorphous Silicon*; Tanaka, K., Ed.; Kluwer: Boston, 1989; Chapter 4.
(16) Tsai, C. C.; Anderson, G. B.; Thompson, R. *J. Non-Cryst. Solids* **1991**, *137*, *138*, 673.
(17) Hishikawa, Y.; Tsuge, S.; Nakamura, N.; Tsuda, S.; Nakano, S.; Kuwano, Y. *J. Appl. Phys.* **1991**, *69*, 508.
(18) Parsons, G. P.; Boland, J. J.; Tsang, J. C. *Jpn. J. Appl. Phys.* **1992**, *31*, 1943.
(19) Shimizu, I. *J. Non-Cryst. Solids* **1989**, *114*, 145. Shirai, H.; Das, D.; Hanna, J.; Shimizu, I. *Appl. Phys. Lett.* **1991**, *59*, 1096. Shirai, H.; Hanna, J.; Shimizu, I. *Jpn. J. Appl. Phys.* **1991**, *30*, L679.
(20) Nguyen, H. V.; An, I.; Collins, R. W.; Lu, Y.; Wakagi, M.; Wronski, C. R. *Appl. Phys. Lett.* **1994**, *65*, 3335.
(21) An, I.; Li, Y. M.; Wronski, C. R.; Collins, R. W. *Phys. Rev. B* **1993**, *48*, 4464.
(22) Gertkemper, T.; Ristein, J.; Ley, L. *J. Non-Cryst. Solids* **1991**, *164*−*166*, 123.
(23) Chabal, Y. J. *Surf. Sci. Rep.* **1988**, *8*, 211.
(24) Chabal, Y. J.; Raghavachari, K. *Phys. Rev. Lett.* **1985**, *54*, 1055. Burrows, V. A.; Chabal, Y. J.; Higashi, G. S.; Raghavachari, K.; Christman, S. B. *Appl. Phys. Lett.* **1988**, *53*, 998.
(25) On the mechanism of the hydrogen-induced exfoliation of silicon. Weldon, M. K.; Marsico, V. E.; Chabal, Y. J.; Agarwal, A.; Eaglesham, D. J.; Sapjeta, J.; Brown, W.; Jacobson, D.; Caudano, Y.; Christman, S. B.; Chaban, E. E. *J. Vac. Sci. Technol. B* **1997**, *15*, 1065.
(26) Jansson, U.; Uram, K. J. *J. Chem. Phys.* **1989**, *91*, 7978.
(27) Uram, K. J.; Jansson, U. *J. Vac. Sci. Technol.* **1989**, *B7*, 1176.
(28) Crowell, J. E.; Lu, G. *J. Electron Spect. Relat. Phenom.* **1990**, *54*, *55*, 1045.
(29) Lee, S. S.; Kong, M.; Bent, S. F.; Chiang, C.-M.; Gates, S. M. *J. Phys. Chem.* **1996**, *100*, 20015.
(30) Gates, S. M.; Kunz, R. R.; Greenlief, C. M. *Surf. Sci.* **1989**, *207*, 364.
(31) Schulze, G.; Henzler, M. *Surf. Sci.* **1983**, *124*, 336.
(32) Street, R. A.; Tsai, C. C.; Kakalios, J.; Jackson, W. B. *Phil. Mag. B* **1987**, *56*, 305.
(33) Fabry, L.; Potzinger, P.; Reimann, B.; Ritter, A.; Steenbergen, H. P. *Organometallics* **1986**, *5*, 1231.
(34) Dobbs, K. D.; Doren, D. J. *J. Am. Chem. Soc.* **1993**, *115*, 3731.
(35) Chiang, C.-M.; Gates, S. M. To be published.

(36) Kulkarni, S. B.; Gates, S. M.; Scott, B. A.; Sawin, H. H. *Surf. Sci.* **1990**, *239*, 13.
(37) Partial Pressure Measurement in Vacuum Technology. Balzers Document No. BG 800 169 PE (8407).
(38) Glass, J. A., Jr.; Wovchko, E. A.; Yates, J. T., Jr. *Surf. Sci.* **1996**, *348*, 325.
(39) Zanzucchi, P. J. The Vibrational Spectra of a-Si:H, Chapter 4 In *Hydrogenated Amorphous Silicon, Part B*; Vol. 21 of Semiconductors and Semimetals; Pankove, J. I., Ed.; Academic Press: New York, 1984.
(40) Toyoshima, Y.; Arai, K.; Matsuda, A.; Tanaka, K. *Appl. Phys. Lett* **1990**, *56*, 1540.
(41) Miyazaki, S.; Okamoto, K.; Miyoshi, Y.; Shin, H.; Hirose, M. *Optoelectronics* **1994**, *9*, 337.
(42) Shin, H.; Miyazaki, S.; Hirose, M. *J. Non-Cryst. Solids* **1991**, *137*, *138*, 713.
(43) Durig, J.; Church, J. S. *J. Chem. Phys.* **1980**, *73*, 4784.
(44) Toyoshima, Y.; Matsuda, A.; Arai, K. *J. Non-Cryst. Solids* **1993**, *164*−*166*, 103.
(45) Carlson, D. E.; Magee, C. W. *Appl. Phys. Lett.* **1978**, *33*, 81.
(46) Gupta, P.; Colvin, V. L.; George, S. M. *Phys. Rev. B* **1988**, *B37*, 8234.
(47) Gates, S. M.; Greenlief, C. M.; Beach, D. B. *J. Chem. Phys.* **1990**, *93*, 7493.
(48) Jasinski, J. M. *Chem. Phys. Lett.* **1993**, *211*, 564.
(49) Naitoh, M.; Morioka, H.; Shoji, F.; Oura, K. *Surf. Sci.* **1993**, *297*, 135.
(50) Abelson, J. R.; Doyle, J. R.; Mandrell, L.; Myers, A. M.; Maley, N. *J. Vac. Sci. Technol. A* **1990**, *A8*, 1364.
(51) Katiyar, M.; Yang, Y. H.; Abelson, J. R. *J. Appl. Phys.* **1995**, *77*, 6247.
(52) Srinivasan, E.; Yang, H.; Parsons, G. N. *J. Chem. Phys.* **1996**, *105*, 5467.
(53) Koehler, B. G.; Mak, C. H.; Arthur, D. A.; Coon, P. A.; George, S. M. *J. Chem. Phys.* **1988**, *89*, 1709.
(54) Walsh, R. Thermochemistry, Chapter 5 In *The Chemistry of Organic Silicon Compounds*; Patai, S., Rappoport, Z., Eds.; Wiley: New York, 1989.
(55) Lin, G. H.; Doyle, J. R.; He, M.; Gallagher, A. *J. Appl. Phys.* **1988**, *64*, 188.
(56) Harris, J.; Kasemo, B. *Surf. Sci.* **1981**, *105*, L281.
(57) Perrin, J. *J. Non-Cryst. Solids* **1991**, *137*, *138*, 639.